

AD-A281 795



KEEP THIS COPY FOR REPRODUCTION PURPOSES

ATION PAGE

Form Approved

OMB No. 0704-0188

average 1 hour per response, including the time for reviewing instructions, searching existing data sources, gathering the collection of information. Send comments regarding this burden estimate or any other aspect of this form to Washington Headquarters Services, Directorate for Information Operations and Reports, 1215 Jefferson Avenue, Management and Budget, Paperwork Reduction Project (0704-0188), Washington, DC 20503.

1. AGENCY USE ONLY (Leave blank)		2. REPORT DATE		3. REPORT TYPE AND DATES COVERED Reprint	
4. TITLE AND SUBTITLE Title shown on Reprint				5. FUNDING NUMBERS DAAL03-92-G-0329 (1)	
6. AUTHOR(S) Author(s) listed on Reprint				DTIC ELECTE JUL 13 1994 S F D	
7. PERFORMING ORGANIZATION NAME(S) AND ADDRESS(ES) University of Arizona Tucson, AZ 85721					
9. SPONSORING/MONITORING AGENCY NAME(S) AND ADDRESS(ES) U. S. Army Research Office P. O. Box 12211 Research Triangle Park, NC 27709-2211				8. PERFORMING ORGANIZATION REPORT NUMBER	
10. SPONSORING/MONITORING AGENCY REPORT NUMBER ARO 30482.9-PH				11. SUPPLEMENTARY NOTES The view, opinions and/or findings contained in this report are those of the author(s) and should not be construed as an official Department of the Army position, policy, or decision, unless so designated by other documentation.	
12a. DISTRIBUTION/AVAILABILITY STATEMENT Approved for public release; distribution unlimited.				12b. DISTRIBUTION CODE	
13. ABSTRACT (Maximum 200 words) ABSTRACT ON REPRINT DTIC QUALITY INSPECTED 8 94-21460 					
14. SUBJECT TERMS				15. NUMBER OF PAGES	
				16. PRICE CODE	
17. SECURITY CLASSIFICATION OF REPORT UNCLASSIFIED		18. SECURITY CLASSIFICATION OF THIS PAGE UNCLASSIFIED		19. SECURITY CLASSIFICATION OF ABSTRACT UNCLASSIFIED	
				20. LIMITATION OF ABSTRACT UL	

NSN 7540-01-280-5500

94 7 12 1 78

Standard Form 298 (Rev. 2-89)
Prescribed by ANSI Std. Z39-18
298-102

Theory of carrier heating through injection pumping and lasing in semiconductor microcavity lasers

F. Jahnke and S. W. Koch

Optical Sciences Center, University of Arizona, Tucson, Arizona 85721

Received April 9, 1993

Nonequilibrium carrier distributions in microcavity lasers are computed by solution of a quantum Boltzmann equation that includes carrier-carrier, carrier-phonon, and carrier-photon scattering as well as the pump process. A significant heating of the carrier plasma is observed as a consequence of the Pauli blocking of carrier injection and the removal of cold carriers through the process of stimulated recombination.

The emission characteristics of semiconductor lasers are governed by the frequency-dependent modal gain and spontaneous emission. In microscopic theory, gain and spontaneous emission are explicit functions of the momentum probability distributions of the electrons and holes.¹ These carrier distributions are determined by the interplay between the pump process, intraband carrier scattering, and stimulated and spontaneous recombination.

If the carrier generation occurs through carrier injection, the carriers can be assumed to have thermalized with the lattice by the time they arrive at the active region. Hence the pump-generated distribution function can be approximated by a quasi-equilibrium Fermi-Dirac distribution at the lattice temperature. At the beginning of the pump process, all carrier states in the previously unexcited laser region are empty and can be populated. However, as soon as the bands are partially filled, Pauli blocking becomes effective, and the pumping is gradually blocked. Since this blocking is more efficient for energetically lower states, the main kinetic energy of excited carriers increases.

During the pump process the carriers in the laser region are constantly redistributed into thermal distributions by the very fast carrier-carrier Coulomb scattering that leads to scattering times of ~ 100 fs.² However, since this elastic-scattering process does not dissipate kinetic energy, the carrier system equilibrates at a temperature that is higher than that of the lattice. Energy from the carrier system is transferred to the lattice through the carrier-phonon coupling. Even though electron-hole scattering tends to equalize the temperature between these two subsystems, the different pump blocking may result in different effective temperatures for electrons and holes.

Stimulated recombination of carriers that is due to the lasing process occurs in the spectral region in which the carrier system is inverted. Since this inversion region is located just above the (renormalized) band gap, the stimulated emission removes electrons and holes with below-average kinetic energy, which further increases the carrier temperature. Well above threshold, when the stimulated recombination time is comparable to or shorter than the intraband carrier scattering, significant deviations

of the actual carrier distributions from the quasi-equilibrium Fermi-Dirac statistics have been found.³

In this Letter we investigate nonequilibrium carrier distributions in semiconductor lasers. Our analysis is performed for microcavity lasers, since these permit only single-longitudinal-mode operation.⁴ However, the conclusions are also valid for conventional long-cavity lasers. We study the temperature changes of the carrier system and their influence on the stationary and dynamical laser operation by solving a Boltzmann equation for the wave-vector-dependent occupation functions of carriers $f_k^{e,h}$:

$$\frac{\partial}{\partial t} f_k^a = (S_k^a)_{\text{scatt}} + (S_k^a)_{\text{stim}} + (S_k^a)_{\text{spont}} + (S_k^a)_{\text{pump}}. \quad (1)$$

The different rates on the right-hand side of this equation describe the carrier scattering (electron-electron, electron-hole, hole-hole, carrier-LO-phonon, carrier-LA-phonon), the stimulated and spontaneous recombination of carriers that is accompanied by photon emission, as well as the pump process.³ The pump process is modeled by

$$(S_k^a)_{\text{pump}} = \frac{j\eta}{ed} \frac{P_k^a(1 - f_k^a)}{\sum_k P_k^a}, \quad (2)$$

where j , e , d , and η are the pump current, electron charge, thickness of the active region, and geometric quantum efficiency, respectively. The Fermi-Dirac function $P_k^a = \{1 + \exp[(1/kT)(\epsilon_k^a - \mu_a)]\}^{-1}$ describes the energy distribution of carriers arriving in the active region. The chemical potential of electrons and holes $\mu_{e,h}$ depends on the applied electric field, $\epsilon_k^{e,h}$ are the free-particle energies of electrons and holes, and T is the lattice temperature.

Without Pauli blocking, $(1 - f_k^a) \approx 1$, and the total pump rate $1/V \sum_k (S_k^a)_{\text{pump}}$ reduces to $j\eta/ed$. The Pauli-blocking factor decreases the pump efficiency and modifies the energy distribution of excited carriers. It is therefore meaningful to introduce an effective quantum efficiency for electrons and holes, which is the product of the geometric quantum efficiency and the Pauli-blocking factor $(\eta_k^a)_{\text{eff}} = \eta(1 - f_k^a)$. This k -dependent quantum efficiency is close to zero for the electrons in the spectral region of the

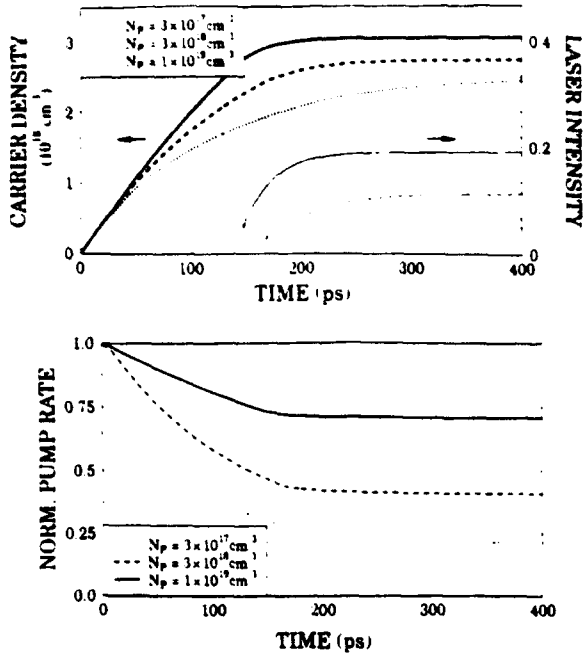


Fig. 1. Time-resolved evolution of carrier density (thick curves), laser intensity (thin curves), and pump rate normalized to $j\eta/ed$ for various energy distribution functions of carriers arriving in the active region $P_k = \{1 + \exp[(1/kT)(\epsilon_k^a - \mu_a)]\}^{-1}$ with lattice temperature $T = 300$ K and density $N_p = 1/V \sum_k P_k$. Zero time corresponds to the onset of the pump process.

gain and approaches the usual quantum efficiency for higher-lying k values.

To compute the nonequilibrium carrier distributions under lasing conditions we have to solve Eq. (1) together with the equation for the spectral light intensity $I(\omega) = 1/V \sum_q I_q(\omega)$,

$$\frac{n(\omega)}{cF_q} \frac{\partial}{\partial t} I_q(\omega) = \left[g(\omega) - \frac{\kappa}{F_q} \right] I_q(\omega) + W(\omega) S_q(\omega), \quad (3)$$

where optical gain $g(\omega)$ and spectral rate of spontaneous emission $W(\omega)$ depend directly on the carrier-momentum-dependent occupation functions of electrons and holes.³ The cavity structure of the laser device modifies the density of state of the various light modes.⁵ In Eq. (3) this leads to a modified loss rate κ/F_q and medium refractive index $n(\omega)/F_q$, where F_q describes the eigenmodes of the laser cavity. The line shape function $S_q(\omega)$ describes the connection between photon wave vectors q and light frequencies ω according to the modified photon-dispersion relation, where $1/V \sum_q S_q(\omega)$ yields the photon density of state.

We numerically solved the coupled Eqs. (1) and (3) for different pump situations, where the initial condition is the unexcited semiconductor and zero intensity inside the cavity. We assume that the pump rate is ramped up to its stationary value within the first picosecond. In Figs. 1 and 2 we compare the cases of different mean kinetic energies of injected carriers, i.e., various chemical potentials $\mu_{e,h}$ in P_k , for otherwise the same conditions to distinguish clearly the influence of pump blocking from the

fact that for the same blocking an increase of the pump current would also increase the temperature. Figure 1 shows the time-resolved density, laser intensity, and pump rate for three different sets of $\mu_{e,h}$ according to the given densities $N_p = 1/V \sum_k P_k$. The corresponding occupation functions of electrons are displayed in Fig. 2 for the stationary situation. For higher chemical potential [higher N_p ; Fig. 2(a)], the effective pump function $(1 - f_k)P_k$ has a peak at larger wave numbers, indicating the preferred pumping of energetically higher states. Correspondingly, we find a strong deviation of the actual carrier occupation f_k from a lattice-temperature Fermi-Dirac distribution with the same carrier density. For low chemical potentials [$N_p = 3 \times 10^{17}$ cm⁻³; Fig. 2(c)], the pumping of carriers according to P_k is restricted to the region of effective blocking. This results in a lower carrier density (Fig. 1, top) because of the less effective pumping (Fig. 1, bottom). Furthermore, it yields a lower effective carrier temperature owing to preferred pumping of energetically lower states. In the presence of the running laser mode, the effective carrier temperature increases further as a consequence of stimulated recombination of cold carriers in a wave-vector region around the laser mode [marked by arrows in Figs. 2(a)–2(c)].

In Figs. 3 and 4 we now analyze the situation in which both the pump current and the chemi-

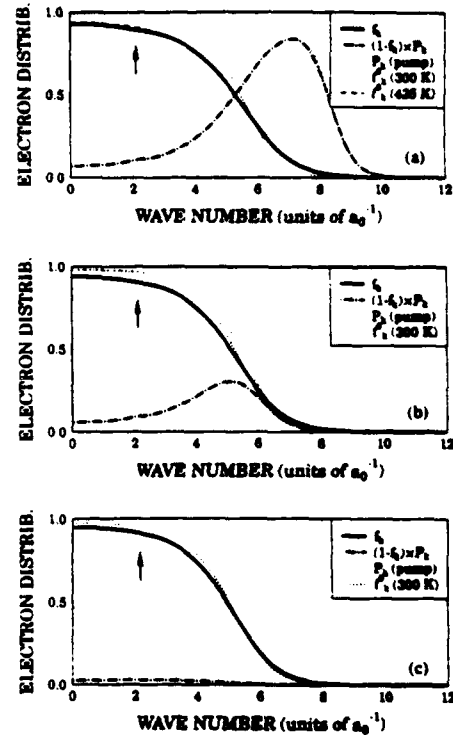


Fig. 2. Momentum-dependent electron distribution functions (solid curves) for the conditions of Fig. 1 after steady-state conditions have been reached. The pump densities are (a) $N_p = 10^{19}$ cm⁻³, (b) $N_p = 3 \times 10^{18}$ cm⁻³, (c) $N_p = 3 \times 10^{17}$ cm⁻³. The dotted curve shows P_k , the dotted-dashed curve is $P_k(1 - f_k)$, and the short-dotted curve shows a Fermi-Dirac distribution function f_k^0 with the same density as f_k and lattice temperature $T = 300$ K. The effective carrier temperatures are (a) 435 K, (b) 390 K, and (c) 355 K.

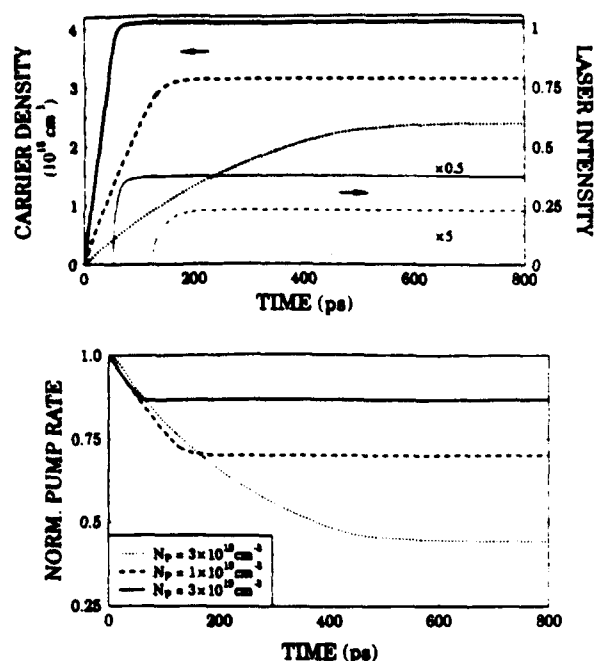


Fig. 3. Time-resolved evolution of carrier density (thick curves), laser intensity (thin curves), and pump rate normalized to $j\eta/ed$ for various pump currents j and carrier distributions P_i . Zero time corresponds to the onset of the pump process.

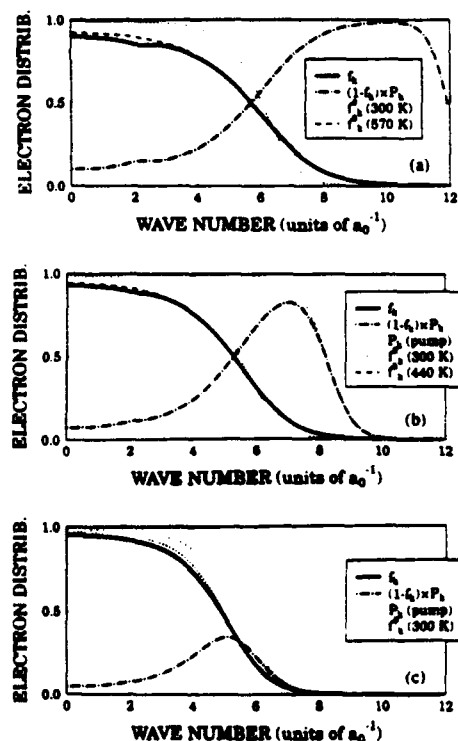


Fig. 4. Stationary electron distribution functions (solid curves) corresponding to Fig. 3 for (a) $N_p = 3 \times 10^{18} \text{ cm}^{-3}$, (b) $N_p = 10^{19} \text{ cm}^{-3}$, and (c) $N_p = 3 \times 10^{19} \text{ cm}^{-3}$. The different curves are as in Fig. 2. The effective carrier temperatures are (a) 570 K, (b) 440 K, and (c) 340 K.

cal potential of the energy distribution of excited carriers P_i change simultaneously. For this pur-

pose we assume that N_p corresponds to the density that would be generated by the pump process alone, i.e., the density generated in the absence of optical transitions. Assuming for simplicity a nonradiative lifetime τ_{nr} of a process proportional to the carrier density, we see that N_p follows from the balance $j\eta/ed = N_p/\tau_{nr}$. Note that the additional consideration of other nonradiative processes, such as Auger recombination, leads to only a shift of the operational point of the laser. Figure 3 shows carrier density, laser intensity, and pump rate for various pump currents $j\eta/ed = 8.7 \times 10^{15}$, 2.9×10^{16} , and $8.7 \times 10^{16} \text{ cm}^{-3} \text{ ps}^{-1}$ and the corresponding pump densities $N_p = 3 \times 10^{18}$, 1×10^{19} , and $3 \times 10^{19} \text{ cm}^{-3}$. Since we now identify higher N_p and, correspondingly, lower pump blocking with increased pump current j , the changes of the stationary laser intensity are even more pronounced than in Fig. 1. In Fig. 4 we see that the preferred pumping of the energetically higher states, accompanied by a higher total pump rate that increases the effective carrier that temperature even more than in the case of Fig. 2. It should be noted that the gain changes that occur as a consequence of carrier heating and hole burning prevent a clamping of the total carrier density for above-threshold pumping levels. This indicates that the carrier density is not a good measure for the modal gain under the discussed conditions.³

This research was supported by the Deutsche Forschungsgemeinschaft, the National Science Foundation, the U.S. Army Research Office, the U.S. Air Force of Scientific Research, and through a grant for CPU time at the Pittsburgh Supercomputer Center. We thank W. Chow of Sandia National Laboratories for useful discussions.

S. W. Koch is also with the Department of Physics, University of Arizona.

References

1. K. Henneberger, F. Jahnke, and F. Herzel, *Phys. Status Solidi B* **173**, 423 (1992); K. Henneberger, F. Herzel, S. W. Koch, R. Binder, A. E. Paul, and D. Scott, *Phys. Rev. A* **45**, 1853 (1992); H. Haug and S. W. Koch, *Phys. Rev. A* **39**, 1887 (1989).
2. D. Scott, R. Binder, and S. W. Koch, *Phys. Rev. Lett.* **69**, 347 (1992); R. Binder, A. E. Paul, D. Scott, K. Henneberger, and S. W. Koch, *Phys. Rev. B* **45**, 1107 (1992).
3. F. Jahnke, K. Henneberger, W. Schäfer, and S. W. Koch, "Transient nonequilibrium and many-body effects in semiconductor microcavity lasers," *J. Opt. Soc. Am. B* (to be published).
4. See, for example, the review by K. Iga, F. Koyanama, and S. Kinoshita, *IEEE J. Quantum Electron.* **24**, 1845 (1988), and the references therein; J. Faist, F. Morier-Genoud, D. Martin, J. A. Ganiere, and F. K. Reinhart, *Electron. Lett.* **24**, 629 (1988); P. L. Gourley, T. M. Brennan, B. E. Hammons, S. W. Corzine, R. S. Geels, R. H. Yam, J. W. Scott, and L. A. Coldren, *Appl. Phys. Lett.* **54**, 1397 (1989).
5. S. Haroche and D. Kleppner, *Phys. Today* **42**(1), 24 (1989).